Geophysical Research Letters

RESEARCH LETTER
10.1029/2024GL113417

Linking Radiative-Advective Equilibrium Regime Transition to Arctic Amplification

Yu-Chiao Liang[1], Osamu Miyawaki[2,3], Tiffany A. Shaw[4], Ivan Mitevski[5], Lorenzo M. Polvani[6,7,8], and Yen-Ting Hwang[1]

[1]Department of Atmospheric Sciences, National Taiwan University, Taipei, Taiwan, [2]Climate and Global Dynamics Laboratory, National Center for Atmospheric Research, Boulder, CO, USA, [3]Geosciences Department, Union College, Schenectady, NY, USA, [4]Department of the Geophysical Sciences, The University of Chicago, Chicago, IL, USA, [5]Department of Geosciences, Princeton University, Princeton, NJ, USA, [6]Lamont-Doherty Earth Observatory, Columbia University, Palisades, NY, USA, [7]Department of Earth and Environmental Sciences, Columbia University, New York, NY, USA, [8]Department of Applied Physics and Applied Mathematics, Columbia University, New York, NY, USA

Key Points:

- Northern high-latitudes undergo considerable climate regime transition in response to varying CO_2 forcing
- Climate regime transition from radiative-advective equilibrium to non-radiative- advective one weakens Arctic amplification (AA)
- Seasonal sea-ice and lapse-rate changes are key processes linking the regime transition to AA

Correspondence to:

Y.-C. Liang,
pamip.yuchiao@gmail.com;
yuchiaoliang@ntu.edu.tw

Citation:

Liang, Y.-C., Miyawaki, O., Shaw, T. A., Mitevski, I., Polvani, L. M., & Hwang, Y.-T. (2025). Linking radiative-advective equilibrium regime transition to Arctic amplification. *Geophysical Research Letters*, *52*, e2024GL113417. https://doi.org/10.1029/2024GL113417

Received 2 NOV 2024
Accepted 7 JAN 2025

Author Contributions:

Conceptualization: Yu-Chiao Liang, Osamu Miyawaki, Tiffany A. Shaw, Ivan Mitevski, Yen-Ting Hwang
Funding acquisition: Yu-Chiao Liang
Investigation: Yu-Chiao Liang, Ivan Mitevski, Yen-Ting Hwang
Methodology: Yu-Chiao Liang, Osamu Miyawaki, Tiffany A. Shaw, Ivan Mitevski, Yen-Ting Hwang
Supervision: Osamu Miyawaki, Tiffany A. Shaw, Lorenzo M. Polvani
Validation: Yu-Chiao Liang
Visualization: Yu-Chiao Liang
Writing – original draft: Yu-Chiao Liang
Writing – review & editing: Yu-Chiao Liang, Osamu Miyawaki, Tiffany A. Shaw, Ivan Mitevski, Lorenzo M. Polvani, Yen-Ting Hwang

Abstract Emission of anthropogenic greenhouse gases has resulted in greater Arctic warming compared to global warming, known as Arctic amplification (AA). From an energy-balance perspective, the current Arctic climate is in radiative-advective equilibrium (RAE) regime, in which radiative cooling is balanced by advective heat flux convergence. Exploiting a suite of climate model simulations with varying carbon dioxide (CO_2) concentrations, we link the northern high-latitude regime variation and transition to AA. The dominance of RAE regime in northern high-latitudes under CO_2 reduction relates to stronger AA, whereas the RAE regime transition to non-RAE regime under CO_2 increase corresponds to a weaker AA. Examinations on the spatial and seasonal structures reveal that lapse-rate and sea-ice processes are crucial mechanisms. Our findings suggest that if CO_2 concentration continues to rise, the Arctic could transition into a non-RAE regime accompanied with a weaker AA.

Plain Language Summary Anthropogenic greenhouse gases have caused dramatic changes in the northern high-latitudes. Specifically, the Arctic climate has experienced significantly greater warming compared to the global mean in recent decades when greenhouse gases concentration increases in the atmosphere. This phenomenon, known as Arctic amplification (AA), is expected to continue according to global climate model simulations. From an energy-balance perspective, the Arctic cooling caused by radiation emitted to space is primarily offset by the heat brought by the atmospheric circulation. This energy-balanced climate regime is called radiative-advective equilibrium (RAE). In this study, we attempt to link AA strength to the Arctic climate regime variation under warming and cooling scenarios. Our findings indicate that in a cooling world, the Arctic is predominantly in the RAE regime, corresponding to a stronger AA. Conversely, in a warming world, the RAE regime gradually transition to non-RAE regime, accompanied with a weaker AA. We also examine the seasonal and spatial structure of climate regime variation, identifying the key processes including changes in sea-ice concentration and vertical temperature profile in the atmosphere. Our results offer a new perspective for studying the rapidly changing Arctic climate.

1. Introduction

Anthropogenic climate change exhibits a remarkable spatial distribution, with amplified surface warming emerging in the Arctic compared to warming elsewhere. This phenomenon is known as Arctic amplification (AA, Previdi et al., 2020; M. C. Serreze & Barry, 2011; Taylor et al., 2022), recorded in palaeoclimate proxies (CAPE-Last Interglacial Project, 2006; Hoffert & Covey, 1992; Miller et al., 2010; Park et al., 2019), observed in historical data (Chapman & Walsh, 1993; England et al., 2021; M. Serreze et al., 2009), and simulated in global climate models (Hahn et al., 2021; Holland & Bitz, 2003; Holland & Landrum, 2021; Manabe & Stouffer, 1980). While the Intergovernmental Panel on Climate Change reported the degree of AA ranging between two and three based on observations and climate model simulations (Lee et al., 2023), recent studies suggested that an alarming threefold to fourfold AA could be occurring (Chylek et al., 2022; Rantanen et al., 2022; W. Zhou et al., 2024). AA not only exerts profound influences on Arctic weather and ecosystem (Alvarez et al., 2020; Burgass et al., 2019; Meredith et al., 2019; Wassmann et al., 2011; Whiteman & Yumashev, 2018), but also has been suggested to affect mid-latitude weather and climate via altering large-scale atmospheric circulations (Cohen et al., 2018; Deser

et al., 2010; England et al., 2020; Francis & Vavrus, 2012; Liang et al., 2024; Screen, 2014; Smith et al., 2022; Sun et al., 2015; Y. Wu & Smith, 2016). Therefore, advancing our mechanistic understanding of AA is crucial for its regional and global socioeconomic implications.

From an energetic perspective, atmospheric radiative cooling in high-latitudes is principally balanced by the advective heat fluxes from lower latitudes in current climate, whereas the surface turbulent fluxes play a lesser role (Nakamura & Oort, 1988; Oort, 1974). This climate regime is referred to as radiative-advective equilibrium (RAE, Cronin & Jansen, 2016). In contrast, the energy balance in low-latitudes is primarily sustained by radiative cooling and surface turbulent fluxes (Riehl & Malkus, 1958), known as radiative-convective equilibrium (RCE, Manabe & Wetherald, 1967; Wing et al., 2018). In the mid-latitudes, all three processes — radiative cooling, heat advection, and surface turbulent fluxes — are important, leading to a climate regime called radiative-convective-advective equilibrium (RCAE, Miyawaki et al., 2022, 2023). The RAE, RCE, and RCAE regimes, respectively, characterize the high-, low-, and mid-latitude climates, and are connected to the surface inversion, moist adiabatic, and mixed lapse-rate regimes (Miyawaki et al., 2022).

More intriguingly, when the climate mean state varies, the regional climate experiences a regime transition. For example, northern high-latitudes can transition from RAE to RCAE regimes in warming scenarios, along with the changes in atmospheric vertical thermal structure (Miyawaki et al., 2023). Meanwhile, AA magnitude presents a mean-state dependence: the strength of AA decreases in a warmer state than in a colder state (Kay et al., 2024; Ono et al., 2022; S.-N. Zhou et al., 2023). These previous findings reveal a possible linkage between the Arctic energy-balance regime transition and AA, which has not been explored thoroughly.

The purpose of this study is to investigate the linkage between the climate regime variation and transition in the northern high-latitudes and AA, building upon a framework proposed by Miyawaki et al. (2022). This framework not only characterizes RAE, RCAE, and RCE regimes, but also quantifies the regime variation and transition to enhance the mechanistic understanding. We utilize a suite of abrupt CO_2 experiments, forced by a wide range of CO_2 forcings (Mitevski, Orbe, et al., 2021), to examine the variations in AA and climate regime. Given that previous studies have highlighted the unique AA seasonal evolution (Hahn et al., 2022; Liang et al., 2022; Y.-T. Wu et al., 2023) and the seasonal RAE-RCAE transitions in high-latitudes (Miyawaki et al., 2022), we further analyze the climate regime variation and transition at seasonal timescale, illustrating the underlying mechanism. We anticipate that the results would offer a new perspective on studying the rapidly changing Arctic climate and the cause of AA, based on the transition in the Arctic energy-balance regime.

2. Data and Methods

In this study, we analyze a suite of 150-year abrupt CO_2 simulations using the fully coupled atmosphere-ocean-sea-ice-land configuration of the Community Earth System Model version 1 (CESM1, Kay et al., 2015). The simulations, with nominal 1° horizontal resolution, follow the protocol for the Coupled Model Intercomparison Project Phase 6 (CMIP6, Eyring et al., 2016). In each simulation set, the CO_2 concentration is fixed throughout the integration period, ranging from one-eighth times the preindustrial (PI) level (i.e., $0.125xCO_2$) to eight times the PI level (i.e., $8xCO_2$). The details of model components and experimental design were documented in previous studies (e.g., Mitevski, Orbe, et al., 2021; Mitevski et al., 2022; S.-N. Zhou et al., 2023). For simplicity, we use $nxCO_2$ run to denote these simulations, where $n = 0.125, 0.25, 0.5, 1, 2, 3, 4, 5, 6, 7$, and 8. We focus on the deviation of any variable from its PI control run (i.e., the $1xCO_2$ run, CO_2 concentration level is fixed at 284.7 ppmv), and define "d(X)" as the difference of variable X in the $nxCO_2$ run and the $1xCO_2$ run. We average the deviation over the last 30 years to represent mean climate response, and refer it to 'response' hereafter. We note that in the $4xCO_2$ run, the shutdown of Atlantic meridional overturning circulation (AMOC) causes abrupt changes in global and Arctic climates. In the runs with higher CO_2 levels, the effect of AMOC shutdown is offset by that of radiative forcing. The relevant analyses and discussion can be found in previous studies (Liang et al., 2022; Mitevski, Orbe, et al., 2021).

The main purpose of this study is to link the energy-balance regime variation and transition to AA. To quantify the strength of AA in the $nxCO_2$ runs, we calculate a unit-less factor (hereafter AAF):

$$\mathrm{AAF} = \frac{\mathrm{dSAT}_{Arctic}}{\mathrm{dSAT}_{global}}, \tag{1}$$

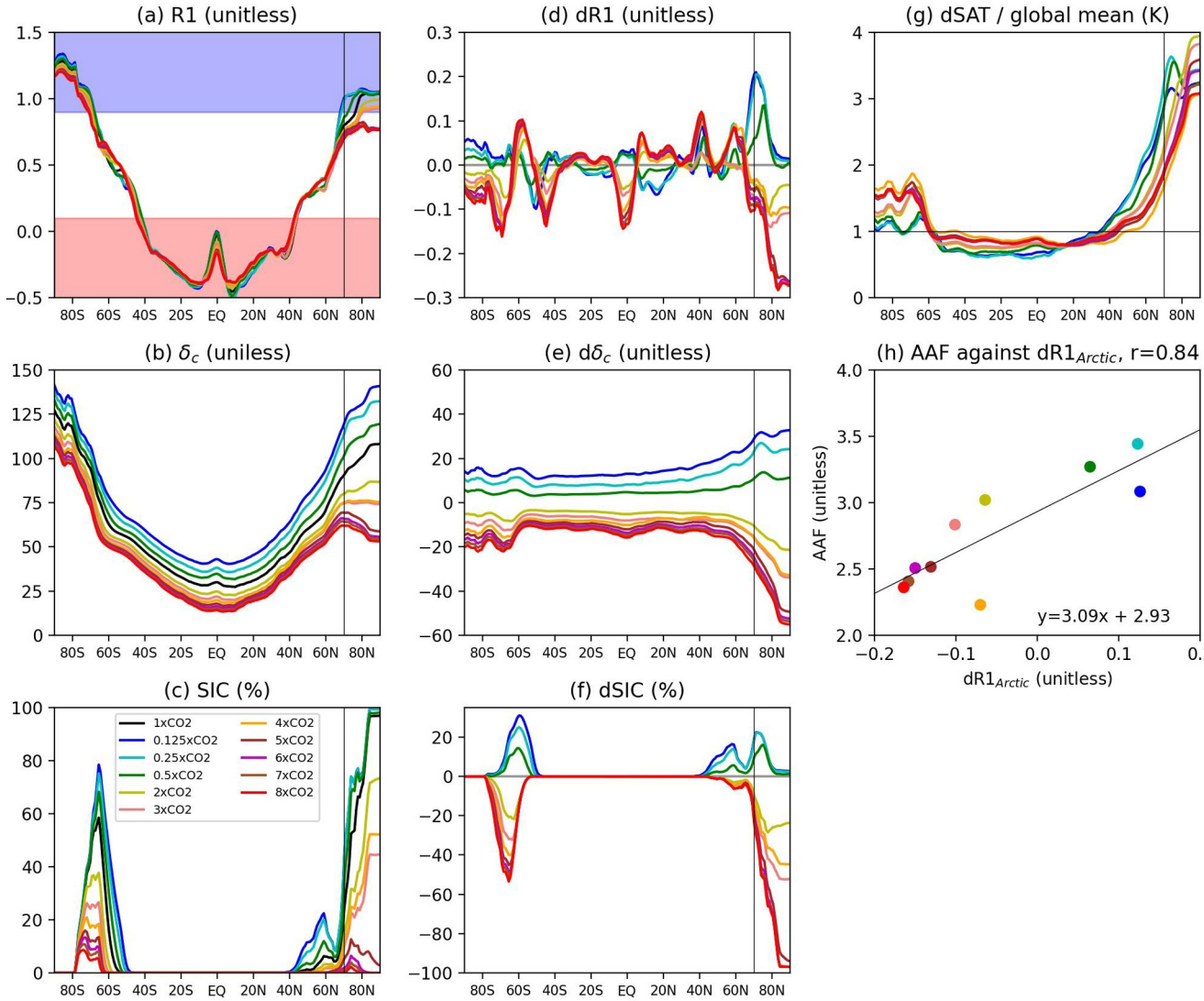

Figure 1. The latitudinal distributions for annual-mean zonal-mean (a) R_1, (b) δ_c, (c) SIC, (d) dR_1, (e) dδ_c, (f) dSIC, (g) dSAT divided by global means, and (h) AAF against dR_1. The purple, white, and red shadings in panel (a) depict the RAE, RCAE, and RCE regimes, respectively. The units are denoted in the title of each panel.

where dSAT$_{Arctic}$ denotes the near-surface air temperature (hereafter SAT) response averaged over the Arctic domain (70° −90°N), while dSAT$_{global}$ denotes the global-averaged SAT response. We chose the southern boundary of the Arctic to be 70°N because evident climate regime variation and large sea-ice change occur to the north of 70°N (Figure 1). However, we conduct the same analysis with the Arctic boundary 60°N and obtain very similar results (not shown). Previous AA studies also adopted similar AAF definition, that is, the ratio metric, and discussed its physical interpretation (e.g., Liang et al., 2022; S.-N. Zhou et al., 2023). It is noted that AAFs for the 0.125xCO_2, 0.25xCO_2, and 0.5xCO_2 runs quantify the amplified Arctic cooling relative to the global cooling.

To understand the characteristics of the climate regimes and quantify the regime variation and transition, we consider the vertically integrated (from the surface layer to model top), zonal-mean moist static energy (MSE) budget:

$$\partial_t m + \partial_y(vm) = R_a + LH + SH, \tag{2}$$

where $m = c_P T + gz + Lq$ is MSE (Neelin & Held, 1987), R_a represents atmospheric radiative cooling, defined as the difference between the radiative fluxes at the top of atmosphere and the surface (by the sign definition,

cooling corresponds to negative value), and *LH* and *SH* correspond to latent and sensible heat fluxes. We next follow Miyawaki et al. (2022) to nondimensionalize Equation 2 by dividing the radiative cooling term R_a on both sides:

$$\underbrace{\frac{\partial_t m + \partial_y(vm)}{R_a}}_{R_1} = 1 + \underbrace{\frac{LH + SH}{R_a}}_{R_2}, \tag{3}$$

where R_1 and R_2 are nondimensional numbers. We use R_1 to define the three energy balance regimes: (a) RAE regime if $R_1 \geq 0.9$, (b) RCE regime if $R_1 \leq 0.1$, and (c) RCAE regime if $0.1 < R_1 < 0.9$. For the RAE regime, $R_1 \geq 0.9$ corresponds to energy balance held by the radiative cooling and MSE convergence. They are almost equally important in this regime, thus their ratio is close to one. From the R_2 perspective, the turbulent fluxes are much weaker than the radiative cooling in this regime, leaving R_2 rather small. For the RCE regime, the energy balance is largely sustained by the turbulent heat fluxes and the radiative cooling, so their ratio is close to minus one and R_1 value is small. The RCAE regime is maintained by all three processes, and corresponds to R_1 values between 0.1 and 0.9. Analyzing the change in R_1, thus, can quantify the regime variation. The physical interpretation of the selected R_1 values to distinguish these climate regimes is discussed in Miyawaki et al. (2022). The threshold values were determined based on reanalysis products, and were validated to apply in climate model simulations. More details and relevant discussion can be found in Section 2a of Miyawaki et al. (2022).

To investigate the underlying mechanism leading to the climate regime variation and transition, we follow Miyawaki et al. (2022) to decompose the seasonality of dR_1 as below:

$$dR_1 = \overline{R_1}\left\{\frac{d(\partial_t m + \partial_y(vm))}{\overline{\partial_t m + \partial_y(vm)}} - \frac{dR_a}{\overline{R_a}}\right\} + \text{Residual}, \tag{4}$$

where the overbar denotes the annual-mean value. The first term quantifies the dynamic contribution, including advection and atmospheric storage, while the second term quantifies the effect of radiative cooling. The third term is the residual, which presents the nonlinear interactions and is overall small but not negligible. We will discuss the effect of residual in the discussion section.

We follow Stone and Carlson (1979) to compute the lapse-rate departure from the moist adiabat as the fractional difference:

$$\delta_c = \frac{\Gamma_m - \Gamma}{\Gamma_m} \times 100\%, \tag{5}$$

where Γ is the actual lapse rate and Γ_m is the corresponding moist adiabatic lapse rate. We compute the vertically integrated δ_c from the surface to the model top. Smaller δ_c value corresponds to the moist adiabatic lapse-rate regime, while larger value denotes the surface inversion lapse-rate regime (Miyawaki et al., 2022).

3. Results

To explore the linkage between high-latitude regime variation, we begin with characterizing the RAE, RCAE, and RCE regimes via analyzing the annual-mean latitudinal distribution of R_1 in the nxCO_2 runs (Figure 1a). One remarkable feature immediately stands out: R_1 varies evidently to a great extent in the northern high-latitudes, whereas it varies less elsewhere. Specifically, most regions of Arctic are in the RAE regime when CO_2 level is reduced with respect to the PI level (lines with cold colors in Figure 1a). In the 2x, 3x, 4xCO_2 runs, RAE regime recedes to higher latitudes, and when CO_2 level continues to elevate, the Arctic becomes completely RAE-free, or, in other words, the Arctic enters the RCAE regime. The response of R_1 (i.e., dR_1) quantifies that R_1 changes in the northern high-latitudes can be twice larger than those in the lower latitudes (Figure 1d). A similar feature also appears in δ_c and dδ_c (Figures 1b and 1e), reflecting the close connection between the climate regime and the lapse-rate regime that was identified in Miyawaki et al. (2022).

As sea ice is required for the maintenance of RAE regime (Miyawaki et al., 2022) and crucial for AA generation (Chung et al., 2021; Dai et al., 2019; Liang et al., 2022), we look into the spatial distributions of annual-mean sea-ice concentration (SIC) and its response (Figures 1c and 1f). As expected, the spatial distribution of dSIC (Figure 1f) corresponds fairly well to that of dR_1 in the northern high-latitudes (Figure 1d). The center of action resides near 70°N, where both CO_2 reduction and increase runs present large dSIC that coincides with large dR_1. In the southern high-latitudes, despite large dSIC and its spatial correspondence to dR_1, dR_1 is not large enough to shift RAE to RCAE regime (Figure 1a). We will discuss the muted regime variation in the southern high-latitudes in the discussion section.

Having shown the spatial consistency between sea-ice, lapse-rate, and energy-balance regime variations, we step further to explore the linkage to AA. The spatial distributions of dSAT normalized by the global mean in the $nxCO_2$ runs show clear polar-amplified signals (values larger than 1, Figure 1g) with their peaks corresponding strikingly well to the peaks or troughs of dR_1 in the northern high-latitudes (c.f., Figure 1d). This suggests a close association between AA and high-latitude regime variation. The statistical analysis on the Arctic-averaged dR_1 and AAF reveals a close relationship between AA and the regime variation, as the correlation coefficient between them is as high as 0.84 such that about 71% of the AA changes across the different CO_2 levels can be explained by dR_1 (Figure 1h). However, one should interpret this result with cautions, as the high correlation coefficient does not mean that dR_1 captures all relevant physics leading to AA with clear causality and a reliable predictor for AA. We discuss the above in the discussion section.

To investigate the mechanism leading to the regime variation and transition in the northern high-latitudes, we look into the monthly evolution of zonal-mean profiles of R_1, δ_c, and SIC (Figure 2). We chose the $0.125xCO_2$ and $8xCO_2$ runs to represent the cooling and warming scenarios, respectively. A noticeable contrast in the two runs is the coverage of RAE regime in the northern high-latitudes, circled by the magenta contour lines in Figure 2. In the $0.125xCO_2$ run, RAE regime persists throughout whole year to the north of 65°N; whereas in the $8xCO_2$ run, RAE regime disappears in most months and in most of high-latitudes, except a narrow band centering around 65°N from October to March and a patch to the north of 80°N during July–August period. δ_c shows consistent spatio-temporal structure with slightly phase lead in time (Figures 2b and 2e). For example, in the $8xCO_2$ run, higher δ_c values begin to emerge in May in the northern high-latitudes, about 1 month earlier than R_1 values becoming larger (c.f., Figures 2d and 2e). This indicates that the lapse-rate regime evolution is happening in advance of the RAE regime evolution in the northern high-latitudes.

The SIC shows consistent temporal evolution but with some spatial differences. In the cold scenario, large SIC persists to the north of 70°N throughout the whole year, favorable for the maintenance of RAE regime (Figure 2c). Another band of SIC to the south of 60°N depicts the sea-ice emergence in the Sea of Okhotsk. In the warm scenarios, in contrast, SIC widely disappears in the northern high-latitudes (Figure 2f). Small SIC persists to the north of 60°N from October to June, detrimental for sustaining the RAE regime.

Focusing on the seasonal evolution, in the CO_2 reduction runs, the Arctic-averaged R_1 are in RAE regime throughout the year, except for the $0.5xCO_2$ run in June (Figure 3a). High SIC throughout the year (Figure 3b) sustains the RAE regime. At PI CO_2 level, the SIC is smaller than in the CO_2 reduction runs, hence the R_1 becomes RCAE from May to July, but remains RAE in other months. All CO_2 increase runs shift the RAE regime in Arctic to RCAE regime, along with lower SIC throughout the year, except $2xCO_2$ and $4xCO_2$ (due to abrupt AMOC shutdown) runs during February-May period when SIC is at seasonal peak. We notice that the SIC seasonal cycle tends to lag R_1 seasonal cycle about 2 months. For example, the SIC minimum for $0.5xCO_2$ occurs in August (green line in Figure 3b), while the R_1 minimum in June (green line in Figure 3a). We follow Equation 4 to decompose R1 and find that the seasonal cycle of radiative component is closer to that of SIC (not shown), suggesting that the SIC modulates the climate regimes in high-latitudes mainly via radiative process.

We next show that dR_1 is larger in the cold season than in the warm season (Figure 3c) consistent with the seasonal evolution of $d\delta_c$ (Figure 3e). It is noted that the seasonal peaks of dSIC and $d\delta_c$ occur about 1 month earlier than that of dR_1. For example, in the $0.125xCO_2$ run, the peaks of dSIC and $d\delta_c$ occur in September, while that of dR_1 in October. These seasonal phase variations indicate that sea-ice and lapse-rate processes play driving roles in the RAE regime formation and transition to RCAE regime, in both warming and cooling scenarios.

To further understand the underlying mechanism, we decompose dR_1 into its radiative and dynamical components (Figures 4b and 4c). During the early warm season, from April to July, the dynamical component counteracts the

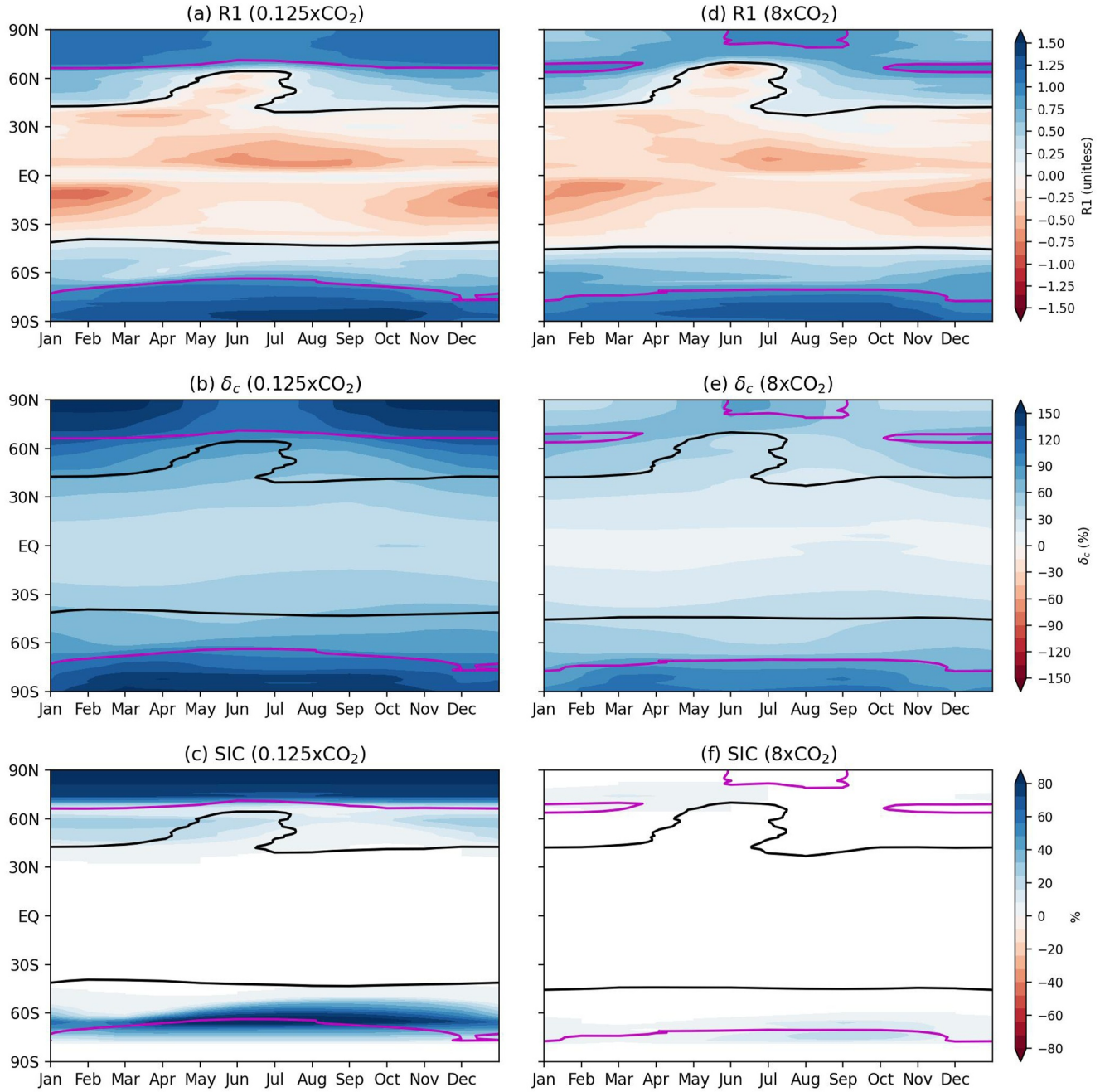

Figure 2. The spatio-temporal evolutions of panel (a) R_1, (b) δ_c, and (c) SIC in 0.125xCO$_2$ run. (d), (e), (f) show the same, but for the 8xCO$_2$ run. The magenta line indicates the boundary between the RAE and RCAE regimes, while the black line denotes the boundary separating the RCAE and RCE regimes.

radiative component, weakening dR_1. In contrast, during other seasons, both components act to intensify dR_1. The seasonal evolution of dR_1 corresponds to that of dynamical component (Figure 4c). We also notice that the annual range of dR_1 is smaller in the CO$_2$ reduction runs compared to that in the CO$_2$ increase runs (Figure 3c), which is also seen in dSIC annual range (Figure 3d). As the radiative component exhibits relatively less variation throughout the year, the dynamical component affects the annual range. This is clearly seen in Figure 4c, where the dynamical component shows larger month-to-month variation, particularly in the cold seasons, in the CO$_2$ increase runs. The residuals are relatively small but not negligible (Figure 4d), indicating that the nonlinear interactions may contribute in particular when the CO$_2$ forcing is weak.

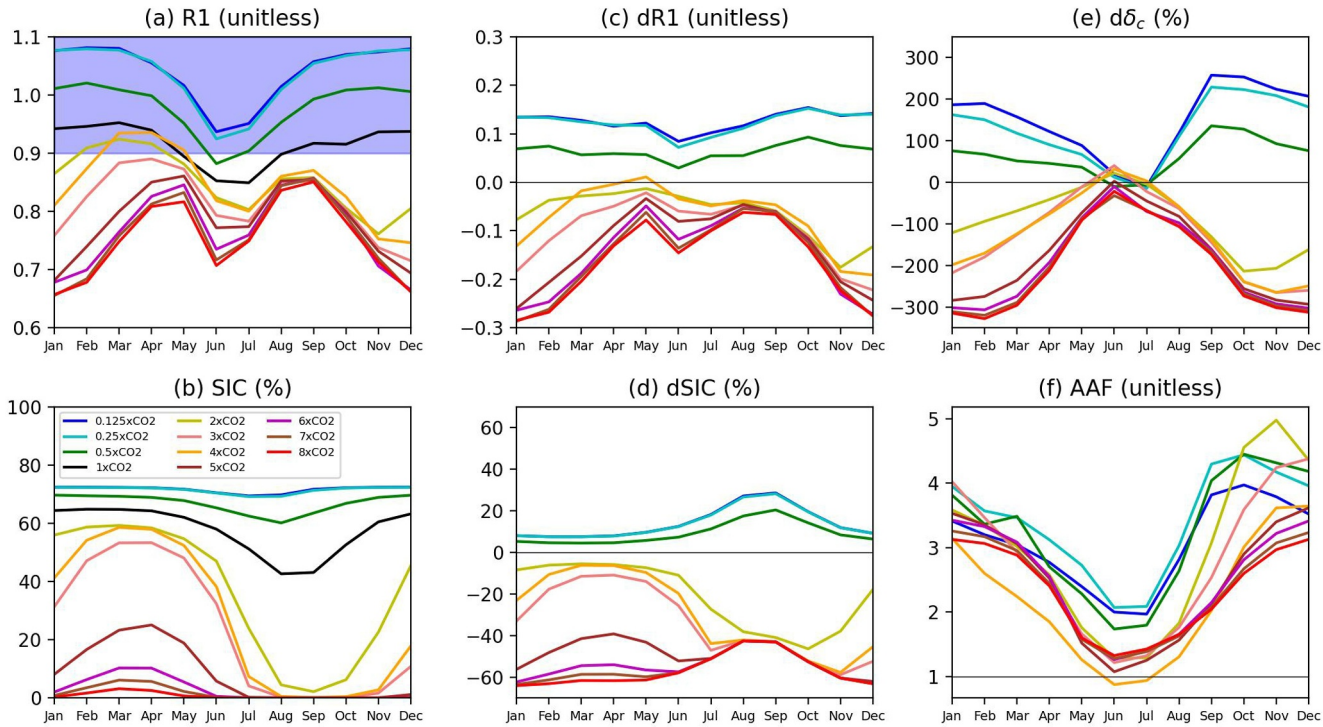

Figure 3. The seasonal evolutions of Arctic-averaged (a) R_1, (b) SIC, (c) dR_1, (d) dSIC, (e) dδ_c, and (f) AAF. The purple and white shadings in (a) indicate the RAE and RCAE regimes, respectively. The units are denoted in the title of each panel.

The above seasonal features of regime variation are consistent with the AAF variation in the CO_2 reduction runs, highlighting their linkage at seasonal timescale. The peak values of AAF and dR_1 coincide in October, while the weakest values occur during June–July period (c.f., Figures 3c and 3f). However, the seasonal cycles of dR_1 and AAF in the CO_2 increase runs show inconsistent evolutions, as the largest dR_1 reduction corresponds to large AAF in the cold seasons. This result suggests that once the Arctic enters RCAE regime due to CO_2 increase, the seasonal correspondence becomes less evident. Furthermore, the annual range of AAF in the CO_2 reduction runs is also smaller than that in the CO_2 increase runs, compatible with the annual range differences of dR_1 in these runs. These findings reflect the close connection between AA and high-latitude climate regime variation at seasonal timescale in RAE regime, and reduced connection when the regime transitions to RCAE.

4. Conclusions and Discussion

This study aims to link the climate regime variation and transition in the northern high-latitudes to the strength of AA using a suite of abrupt CO_2 experiments with a wide range of CO_2 levels, which has not been investigated before. We apply a diagnostic framework proposed by Miyawaki et al. (2022) that can quantify the variation in the RAE, RCAE, and RCE regimes. In a cold scenario due to CO_2 reduction, the northern high-latitudes experience expanded sea-ice coverage, leaving less open ocean and limiting atmosphere-ocean heat fluxes exchange. The energy balance, therefore, is mostly sustained by the radiative cooling and advective heat fluxes convergence, favorable for the RAE regime and the surface inversion lapse-rate regime (Miyawaki et al., 2022). In contrast, increasing CO_2 level, along with sea-ice retreat, leads to an energy balance regime consistent with the RCAE regime and featuring mixed lapse-rate regime. From a process-level perspective, the sea-ice change (e.g., Dai et al., 2019; Chung et al., 2021; Liang et al., 2022; S.-N. Zhou et al., 2023) and the lapse-rate feedback (e.g., Goosse et al., 2018; Pithan & Mauritsen, 2014; S.-N. Zhou et al., 2023), both of which have been considered key mechanisms in generating AA, work together to establish the linkage between regime variation and AA. We conclude that the degree to which RAE regime transitions to RCAE closely links to the strength of AA. It is anticipated that, if CO_2 concentration continues to grow, the Arctic would transition from RAE regime to RCAE regime, resonating the findings in transient climate model simulations (Miyawaki et al., 2023).

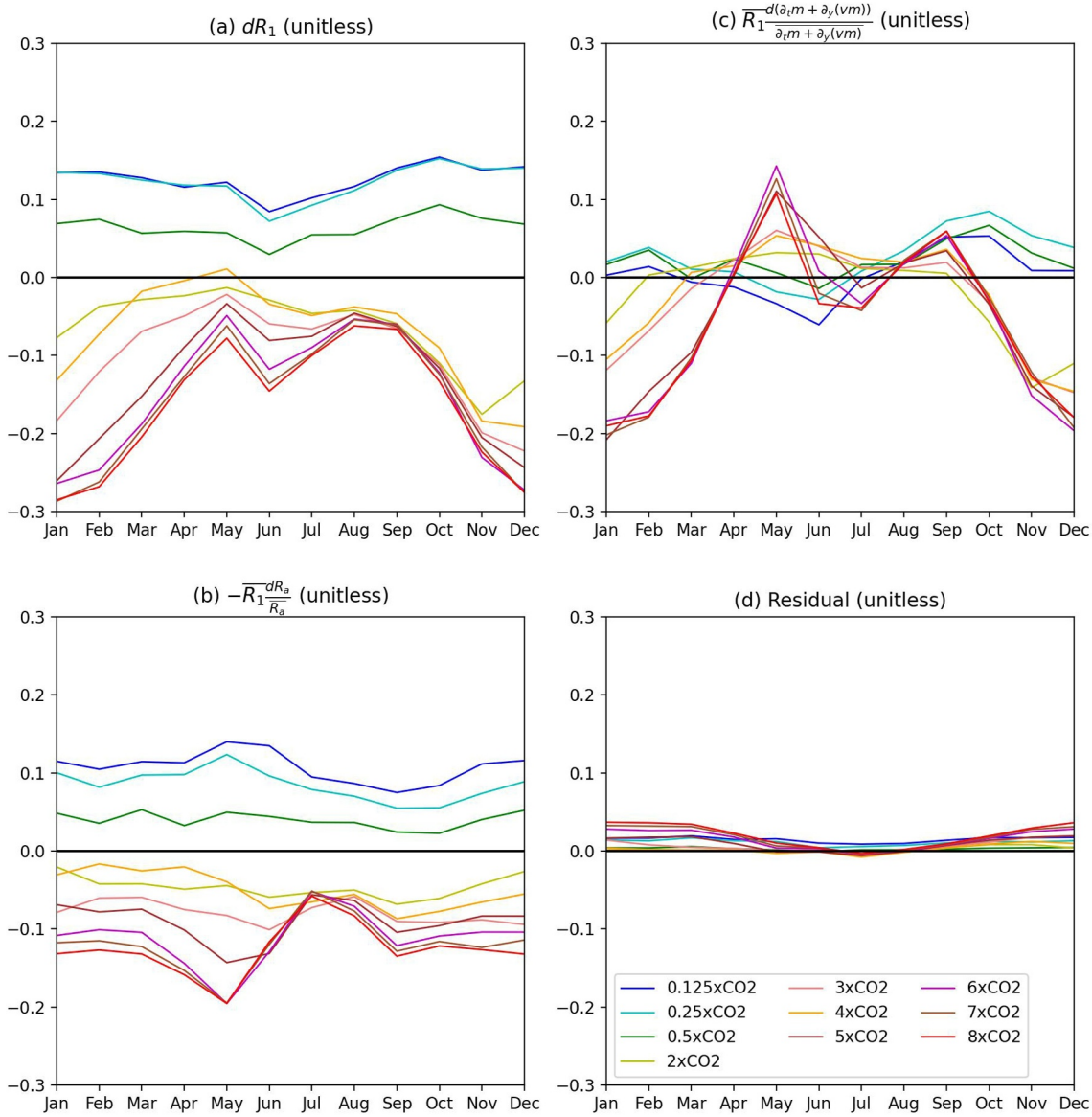

Figure 4. The seasonal evolutions of Arctic-averaged (a) R_1, (b) dynamical component $\left(\overline{R_1}\frac{d(\partial_t m+\partial_y(vm))}{\partial_t m+\partial_y(vm)}\right)$, (c) radiative component $\left(-\frac{dR_a}{\overline{R_a}}\right)$, and (d) residual. The units are denoted in the title of each panel.

Considering that in abrupt CO_2 experiments other climate models are not forced with CO_2 levels more than 4 times the PI level, we may need to take account for other factors aside from the lapse-rate and sea-ice processes. Indeed, when we only use the runs with CO_2 levels less than $4xCO_2$, the correlation coefficient between dR_1 and AAF becomes 0.7, suggesting other process intervenes. If we repeat the same analysis without including the cold runs, the correlation coefficient drops substantially, indicating that in RCAE regime this relationship does not hold. The opposite result emerges in the southern high-latitudes when AAF decreases along with stronger R_1 (Figures 1a and 1g), suggesting this relationship does not apply to Antarctic, either. In the dR_1 decomposition, we also see that the residual term could be similar in magnitude to other components particularly in lower CO_2 levels, suggesting that the effect of nonlinear interactions emerges. One additional analysis to reveal other factors and the nonlinear effect is to follow the feedback-locking analysis (Beer & Eisenman, 2022). This framework allows us to examine the nonlinear interactions between feedbacks and meridional heat transport, which may be crucial when CO_2 forcing turns weak. Another approach could be using the transient runs (Miyawaki et al., 2023), which would shed insights on the mechanism under weaker CO_2 forcing.

Looking into the seasonality changes in the northern high-latitudes reveals a close linkage between high-latitude regime variation and AA at seasonal timescale and the underlying mechanisms. The fact that the peaks of sea-ice and lapse-rate changes occur about 1 month in advance strongly suggests that they are the essential mechanisms establishing the RAE transition-AA linkage. We also notice that, when the Arctic is in RAE regime throughout the seasons, the seasonal cycles of the regime variation and AAF correspond nicely well in the CO_2 reduction runs. This correspondence becomes less evident in the CO_2 increase runs as now the Arctic enters RCAE regime. This result reflect the fundamental difference in the two energy-balance regime and raises some interesting and important questions. For example, what is the physical nature of the RCAE regime? In what way does it differ from the RAE regime, and how do these differences affect AA? Miyawaki et al. (2022) showed that the different lapse-rate regime phenomenologically links to them, but, at least we are aware of, no theoretical framework has been attempted to answer these questions. Cronin and Jansen (2016) provided some physical insights into the RAE regime. Following similar approach, our findings here may offer serve as useful phenomenological reference for future theoretical and process-oriented studies on the RCAE regime.

A notable contrast manifests in the southern high-latitudes. Although the sea-ice changes considerably from cold to warm scenarios (c.f., Figures 2c and 2f), the climate regime does not vary much and stays in RAE (Figure 1a). Indeed, the amplified SAT is stronger in the CO_2 increase runs than that in the reduction runs (Figure 1g), opposite to the northern-hemisphere counterpart. This is likely due to the climate regime variation residing to the south of predominant sea-ice changes, not allowing the atmosphere-ocean heat fluxes to sustain energy balance directly. Smaller spatial change in lapse rate (c.f., Figures 2b and 2e) possibly also weakens the effect of lapse-rate feedback that promotes amplified warming or cooling. Therefore, the energy-balance regime variation is not closely link to the "Antarctic amplification." The high elevation of Antarctic topography has also been suggested as a factor responsible for no Antarctic amplification because of muted lapse-rate feedback (Hahn et al., 2020; Salzmann, 2017), while the contribution of ocean dynamics was investigated (Marshall et al., 2014). Future studies considering their roles should provide further insights.

One more intriguing phenomenon we observe is stronger AA in the cooling scenarios than in the warming scenario (Figure 1f). S.-N. Zhou et al. (2023) conducted a process-based analysis to show that the lapse-rate feedback is the key process for this AA asymmetry. Indeed, the lapse-rate feedback was identified working asymmetrically on polar amplification in cold and warm climates in an idealized model simulation (Merlis et al., 2022) and a comprehensive climate model (Eisenman & Armour, 2024). However, there is a lack of a clear explanation of why the lapse-rate feedback reacts to warming and cooling forcings asymmetrically. Our analysis focusing on energy-balance regime variation and transition may offer an alternative perspective to answer, or at least to shed some insights into, this phenomenon. As discussed above, our results suggest that the response of lapse-rate feedback to warming and cooling forcings in the RAE regime could be fundamentally different from the response in the RCAE regime. Including the surface heat fluxes in the RCAE regime may weaken the effectiveness of lapse-rate feedback by demolishing the surface inversion, resulting in weaker AA. Furthermore, the effect of cloud on the energy balance (Prince & L'Ecuyer, 2024) may be intensified in the RCAE regime but muted in the RAE regime. This could also contribute to the lapse-rate non-linearity and asymmetric AA. These arguments are hypothetical and require further investigations.

Data Availability Statement

The data of CO_2 experiments can be obtained via Mitevski, Polvani, and Orbe (2021). The plotting Python scripts can be downloaded from Liang (2024).

Acknowledgments
We thank three anomalous reviewers for the constructive comments. Y.-C. Liang are supported by Grants from the National Science and Technology council (NSTC 112-2628-M-002-009 and 113-2628-M-002-018). I. Mitevski is supported by a Harry Hess post-doctoral fellowship from Princeton Geosciences. L.M. Polvani acknowledges support from a US NSF Grant. We acknowledge high-performance computing support from Cheyenne (10.5065/D6RX99HX) by NCAR's Computational and Information Systems Laboratory.

References

Alvarez, J., Yumashev, D., & Whiteman, G. (2020). A framework for assessing the economic impacts of arctic change. *Ambio*, *49*(2), 407–418. https://doi.org/10.1007/s13280-019-01211-z

Beer, E., & Eisenman, I. (2022). Revisiting the role of the water vapor and lapse rate feedbacks in the arctic amplification of climate change. *Journal of Climate*, *35*(10), 2975–2988. https://doi.org/10.1175/jcli-d-21-0814.1

Burgass, M. J., Milner-Gulland, E., Stewart Lowndes, J. S., O'Hara, C., Afflerbach, J. C., & Halpern, B. S. (2019). A pan-arctic assessment of the status of marine social-ecological systems. *Regional Environmental Change*, *19*(1), 293–308. https://doi.org/10.1007/s10113-018-1395-6

CAPE-Last Interglacial Project, x. (2006). Last interglacial arctic warmth confirms polar amplification of climate change. *Quaternary Science Reviews*, *25*(13–14), 1383–1400.

Chapman, W. L., & Walsh, J. E. (1993). Recent variations of sea ice and air temperature in high latitudes. *Bulletin of the American Meteorological Society*, *74*(1), 33–48. https://doi.org/10.1175/1520-0477(1993)074<0033:rvosia>2.0.co;2

Chung, E.-S., Ha, K.-J., Timmermann, A., Stuecker, M. F., Bodai, T., & Lee, S.-K. (2021). Cold-season arctic amplification driven by arctic ocean-mediated seasonal energy transfer. *Earth's Future*, *9*(2), e2020EF001898. https://doi.org/10.1029/2020ef001898

Chylek, P., Folland, C., Klett, J. D., Wang, M., Hengartner, N., Lesins, G., & Dubey, M. K. (2022). Annual mean arctic amplification 1970–2020: Observed and simulated by CMIP6 climate models. *Geophysical Research Letters*, *49*(13), e2022GL099371. https://doi.org/10.1029/2022gl099371

Cohen, J., Pfeiffer, K., & Francis, J. A. (2018). Warm arctic episodes linked with increased frequency of extreme winter weather in the United States. *Nature Communications*, *9*(1), 869. https://doi.org/10.1038/s41467-018-02992-9

Cronin, T. W., & Jansen, M. F. (2016). Analytic radiative-advective equilibrium as a model for high-latitude climate. *Geophysical Research Letters*, *43*(1), 449–457. https://doi.org/10.1002/2015gl067172

Dai, A., Luo, D., Song, M., & Liu, J. (2019). Arctic amplification is caused by sea-ice loss under increasing CO_2. *Nature Communications*, *10*(1), 121. https://doi.org/10.1038/s41467-018-07954-9

Deser, C., Tomas, R., Alexander, M., & Lawrence, D. (2010). The seasonal atmospheric response to projected arctic sea ice loss in the late twenty-first century. *Journal of Climate*, *23*(2), 333–351. https://doi.org/10.1175/2009jcli3053.1

Eisenman, I., & Armour, K. C. (2024). The radiative feedback continuum from snowball earth to an ice-free hothouse. *Nature Communications*, *15*(1), 6582. https://doi.org/10.1038/s41467-024-50406-w

England, M. R., Eisenman, I., Lutsko, N. J., & Wagner, T. J. (2021). The recent emergence of Arctic Amplification. *Geophysical Research Letters*, *48*(15), e2021GL094086. https://doi.org/10.1029/2021gl094086

England, M. R., Polvani, L. M., Sun, L., & Deser, C. (2020). Tropical climate responses to projected arctic and Antarctic sea-ice loss. *Nature Geoscience*, *13*(4), 275–281. https://doi.org/10.1038/s41561-020-0546-9

Eyring, V., Bony, S., Meehl, G. A., Senior, C. A., Stevens, B., Stouffer, R. J., & Taylor, K. E. (2016). Overview of the coupled model intercomparison project phase 6 (CMIP6) experimental design and organization. *Geoscientific Model Development*, *9*(5), 1937–1958. https://doi.org/10.5194/gmd-9-1937-2016

Francis, J. A., & Vavrus, S. J. (2012). Evidence linking arctic amplification to extreme weather in mid-latitudes. *Geophysical Research Letters*, *39*(6), L06801. https://doi.org/10.1029/2012gl051000

Goosse, H., Kay, J. E., Armour, K. C., Bodas-Salcedo, A., Chepfer, H., Docquier, D., et al. (2018). Quantifying climate feedbacks in Polar Regions. *Nature Communications*, *9*(1), 1919. https://doi.org/10.1038/s41467-018-04173-0

Hahn, L. C., Armour, K. C., Battisti, D. S., Donohoe, A., Pauling, A., & Bitz, C. M. (2020). Antarctic elevation drives hemispheric asymmetry in polar lapse rate climatology and feedback. *Geophysical Research Letters*, *47*(16), e2020GL088965. https://doi.org/10.1029/2020gl088965

Hahn, L. C., Armour, K. C., Battisti, D. S., Eisenman, I., & Bitz, C. M. (2022). Seasonality in arctic warming driven by sea ice effective heat capacity. *Journal of Climate*, *35*(5), 1629–1642. https://doi.org/10.1175/jcli-d-21-0626.1

Hahn, L. C., Armour, K. C., Zelinka, M. D., Bitz, C. M., & Donohoe, A. (2021). Contributions to polar amplification in CMIP5 and CMIP6 models. *Frontiers in Earth Science*, *9*, 710036. https://doi.org/10.3389/feart.2021.710036

Hoffert, M. I., & Covey, C. (1992). Deriving global climate sensitivity from palaeoclimate reconstructions. *Nature*, *360*(6404), 573–576. https://doi.org/10.1038/360573a0

Holland, M. M., & Bitz, C. M. (2003). Polar amplification of climate change in coupled models. *Climate Dynamics*, *21*(3), 221–232. https://doi.org/10.1007/s00382-003-0332-6

Holland, M. M., & Landrum, L. (2021). The emergence and transient nature of arctic amplification in coupled climate models. *Frontiers in Earth Science*, *9*, 719024. https://doi.org/10.3389/feart.2021.719024

Kay, J. E., Deser, C., Phillips, A., Mai, A., Hannay, C., Strand, G., et al. (2015). The community earth system model (CESM) large ensemble project: A community resource for studying climate change in the presence of internal climate variability. *Bulletin of the American Meteorological Society*, *96*(8), 1333–1349. https://doi.org/10.1175/bams-d-13-00255.1

Kay, J. E., Liang, Y.-C., Zhou, S.-N., & Maher, N. (2024). Sea ice feedbacks cause more greenhouse cooling than greenhouse warming at high northern latitudes on multi-century timescales. *Environmental Research: Climate*, *3*(4), 041003. https://doi.org/10.1088/2752-5295/ad8026

Lee, H., Calvin, K., Dasgupta, D., Krinner, G., Mukherji, A., Thorne, P., et al. (2023). H. Lee & J. Romero (Eds.), *IPCC, 2023: Climate change 2023: Synthesis report, summary for policymakers. Contribution of working groups I, II and III to the sixth assessment report of the intergovernmental panel on climate change [core writing team*. ipcc, geneva.

Liang, Y.-C. (2024). rae−aa−linkage−2024−yuchiaoliang [Software]. *Zenodo*. https://doi.org/10.5281/zenodo.12732424

Liang, Y.-C., Kwon, Y.-O., Frankignoul, C., Gastineau, G., Smith, K. L., Polvani, L. M., et al. (2024). The weakening of the stratospheric polar vortex and the subsequent surface impacts as consequences to arctic sea ice loss. *Journal of Climate*, *37*(1), 309–333. https://doi.org/10.1175/jcli-d-23-0128.1

Liang, Y.-C., Polvani, L. M., & Mitevski, I. (2022). Arctic amplification, and its seasonal migration, over a wide range of abrupt CO_2 forcing. *npj Climate and Atmospheric Science*, *5*(1), 14. https://doi.org/10.1038/s41612-022-00228-8

Manabe, S., & Stouffer, R. J. (1980). Sensitivity of a global climate model to an increase of CO_2 concentration in the atmosphere. *Journal of Geophysical Research*, *85*(C10), 5529–5554. https://doi.org/10.1029/jc085ic10p05529

Manabe, S., & Wetherald, R. T. (1967). Thermal equilibrium of the atmosphere with a given distribution of relative humidity. *Journal of the Atmospheric Sciences*, *24*(3), 241–259. https://doi.org/10.1175/1520-0469(1967)024<0241:teotaw>2.0.co;2

Marshall, J., Armour, K. C., Scott, J. R., Kostov, Y., Hausmann, U., Ferreira, D., et al. (2014). The ocean's role in polar climate change: Asymmetric arctic and antarctic responses to greenhouse gas and ozone forcing. *Philosophical Transactions of the Royal Society A: Mathematical, Physical & Engineering Sciences*, *372*(2019), 20130040. https://doi.org/10.1098/rsta.2013.0040

Meredith, M., Sommerkorn, M., Cassotta, S., Derksen, C., Ekaykin, A., Hollowed, A., et al. (2019). Polar Regions. Chapter 3, IPCC special report on the ocean and cryosphere in a changing climate.

Merlis, T. M., Feldl, N., & Caballero, R. (2022). Changes in poleward atmospheric energy transport over a wide range of climates: Energetic and diffusive perspectives and a priori theories. *Journal of Climate*, *35*(20), 6533–6548. https://doi.org/10.1175/jcli-d-21-0682.1

Miller, G. H., Alley, R. B., Brigham-Grette, J., Fitzpatrick, J. J., Polyak, L., Serreze, M. C., & White, J. W. (2010). Arctic amplification: Can the past constrain the future? *Quaternary Science Reviews*, *29*(15–16), 1779–1790. https://doi.org/10.1016/j.quascirev.2010.02.008

Mitevski, I., Orbe, C., Chemke, R., Nazarenko, L., & Polvani, L. M. (2021a). Non-monotonic response of the climate system to abrupt CO_2 forcing. *Geophysical Research Letters*, *48*(6), e2020GL090861. https://doi.org/10.1029/2020gl090861

Mitevski, I., Polvani, L., & Orbe, C. (2021b). Abrupt and transient CO2 experiments with cesm-le [Dataset]. *Zenodo*. https://doi.org/10.5281/zenodo.5725084

Mitevski, I., Polvani, L. M., & Orbe, C. (2022). Asymmetric warming/cooling response to CO_2 increase/decrease mainly due to non-logarithmic forcing, not feedbacks. *Geophysical Research Letters*, *49*(5), e2021GL097133. https://doi.org/10.1029/2021gl097133

Miyawaki, O., Shaw, T., & Jansen, M. (2023). The emergence of a new wintertime arctic energy balance regime. *Environmental Research: Climate*, *2*(3), 031003. https://doi.org/10.1088/2752-5295/aced63

Miyawaki, O., Shaw, T. A., & Jansen, M. F. (2022). Quantifying energy balance regimes in the modern climate, their link to lapse rate regimes, and their response to warming. *Journal of Climate*, *35*(3), 1045–1061. https://doi.org/10.1175/jcli-d-21-0440.1

Nakamura, N., & Oort, A. H. (1988). Atmospheric heat budgets of the polar regions. *Journal of Geophysical Research*, *93*(D8), 9510–9524. https://doi.org/10.1029/jd093id08p09510

Neelin, J. D., & Held, I. M. (1987). Modeling tropical convergence based on the moist static energy budget. *Monthly Weather Review*, *115*(1), 3–12. https://doi.org/10.1175/1520-0493(1987)115<0003:mtcbot>2.0.co;2

Ono, J., Watanabe, M., Komuro, Y., Tatebe, H., & Abe, M. (2022). Enhanced arctic warming amplification revealed in a low-emission scenario. *Communications Earth & Environment*, *3*(1), 27. https://doi.org/10.1038/s43247-022-00354-4

Oort, A. H. (1974). Year-to-year variations in the energy balance of the arctic atmosphere. *Journal of Geophysical Research*, *79*(9), 1253–1260. https://doi.org/10.1029/jc079i009p01253

Park, H.-S., Kim, S.-J., Stewart, A. L., Son, S.-W., & Seo, K.-H. (2019). Mid-holocene northern hemisphere warming driven by arctic amplification. *Science Advances*, *5*(12), eaax8203. https://doi.org/10.1126/sciadv.aax8203

Pithan, F., & Mauritsen, T. (2014). Arctic amplification dominated by temperature feedbacks in contemporary climate models. *Nature Geoscience*, *7*(3), 181–184. https://doi.org/10.1038/ngeo2071

Previdi, M., Janoski, T. P., Chiodo, G., Smith, K. L., & Polvani, L. M. (2020). Arctic amplification: A rapid response to radiative forcing. *Geophysical Research Letters*, *47*(17), e2020GL089933. https://doi.org/10.1029/2020gl089933

Prince, H. D., & L'Ecuyer, T. S. (2024). Observed energetic adjustment of the arctic and Antarctic in a warming world. *Journal of Climate*, *37*(8), 2611–2627. https://doi.org/10.1175/jcli-d-23-0294.1

Rantanen, M., Karpechko, A. Y., Lipponen, A., Nordling, K., Hyvärinen, O., Ruosteenoja, K., et al. (2022). The arctic has warmed nearly four times faster than the globe since 1979. *Communications Earth & Environment*, *3*(1), 168. https://doi.org/10.1038/s43247-022-00498-3

Riehl, H., & Malkus, J. (1958). On the heat balance in the equatorial trough zone. *Geophysica*, *6*, 503–538.

Salzmann, M. (2017). The polar amplification asymmetry: Role of Antarctic surface height. *Earth System Dynamics*, *8*(2), 323–336. https://doi.org/10.5194/esd-8-323-2017

Screen, J. A. (2014). Arctic amplification decreases temperature variance in northern mid-to high-latitudes. *Nature Climate Change*, *4*(7), 577–582. https://doi.org/10.1038/nclimate2268

Serreze, M., Barrett, A., Stroeve, J., Kindig, D., & Holland, M. (2009). The emergence of surface-based arctic amplification. *The Cryosphere*, *3*(1), 11–19. https://doi.org/10.5194/tc-3-11-2009

Serreze, M. C., & Barry, R. G. (2011). Processes and impacts of arctic amplification: A research synthesis. *Global and Planetary Change*, *77*(1–2), 85–96. https://doi.org/10.1016/j.gloplacha.2011.03.004

Smith, D. M., Eade, R., Andrews, M., Ayres, H., Clark, A., Chripko, S., et al. (2022). Robust but weak winter atmospheric circulation response to future arctic sea ice loss. *Nature Communications*, *13*(1), 727. https://doi.org/10.1038/s41467-022-28283-y

Stone, P. H., & Carlson, J. H. (1979). Atmospheric lapse rate regimes and their parameterization. *Journal of the Atmospheric Sciences*, *36*(3), 415–423. https://doi.org/10.1175/1520-0469(1979)036<0415:alrrat>2.0.co;2

Sun, L., Deser, C., & Tomas, R. A. (2015). Mechanisms of stratospheric and tropospheric circulation response to projected arctic sea ice loss. *Journal of Climate*, *28*(19), 7824–7845. https://doi.org/10.1175/jcli-d-15-0169.1

Taylor, P. C., Boeke, R. C., Boisvert, L. N., Feldl, N., Henry, M., Huang, Y., et al. (2022). Process drivers, inter-model spread, and the path forward: A review of amplified arctic warming. *Frontiers in Earth Science*, *9*, 1391. https://doi.org/10.3389/feart.2021.758361

Wassmann, P., Duarte, C. M., Agusti, S., & Sejr, M. K. (2011). Footprints of climate change in the arctic marine ecosystem. *Global Change Biology*, *17*(2), 1235–1249. https://doi.org/10.1111/j.1365-2486.2010.02311.x

Whiteman, G., & Yumashev, D. (2018). Poles apart: The arctic & management studies. *Journal of Management Studies*, *55*(5), 873–879. https://doi.org/10.1111/joms.12337

Wing, A. A., Reed, K. A., Satoh, M., Stevens, B., Bony, S., & Ohno, T. (2018). Radiative–convective equilibrium model intercomparison project. *Geoscientific Model Development*, *11*(2), 793–813. https://doi.org/10.5194/gmd-11-793-2018

Wu, Y., & Smith, K. L. (2016). Response of northern hemisphere midlatitude circulation to arctic amplification in a simple atmospheric general circulation model. *Journal of Climate*, *29*(6), 2041–2058. https://doi.org/10.1175/jcli-d-15-0602.1

Wu, Y.-T., Liang, Y.-C., Kuo, Y.-N., Lehner, F., Previdi, M., Polvani, L. M., et al. (2023). Exploiting smiles and the CMIP5 archive to understand arctic climate change seasonality and uncertainty. *Geophysical Research Letters*, *50*(2), e2022GL100745. https://doi.org/10.1029/2022gl100745

Zhou, S.-N., Liang, Y.-C., Mitevski, I., & Polvani, L. M. (2023). Stronger arctic amplification produced by decreasing, not increasing, CO2 concentrations. *Environmental Research: Climate*, *2*(4), 045001. https://doi.org/10.1088/2752-5295/aceea2

Zhou, W., Leung, L. R., & Lu, J. (2024). Steady threefold arctic amplification of externally forced warming masked by natural variability. *Nature Geoscience*, *17*(6), 1–8. https://doi.org/10.1038/s41561-024-01441-1